

# Reactor antineutrino anomaly revisited circa 2021

Z. Xin<sup>1,2</sup>

<sup>1</sup>Institute of High Energy Physics, Chinese Academy of Sciences, Beijing 100049, China

<sup>2</sup>School of Physical Sciences, University of Chinese Academy of Sciences, Beijing 100049, China

E-mail: [xinzhaoh@ihep.ac.cn](mailto:xinzhaoh@ihep.ac.cn)

**Abstract.** In our recent work [1], we study the status of the reactor antineutrino anomaly in light of new reactor flux conversion and summation models. We present a new improved calculation of the IBD yields of the standard Huber-Mueller (HM) model and those of the new models. We show that the reactor rates and the fuel evolution data are consistent with the predictions of the Kurchatov Institute (KI) conversion model and with those of the Estienne-Fallot (EF) summation model, leading to a plausible robust demise of the reactor antineutrino anomaly. We also show that the results of several goodness of fit tests favor the KI and EF models over other models under consideration.

## 1 Introduction

Reactor antineutrinos have been widely used to study the fundamental properties of neutrinos [2], which are mainly from beta decays of neutron-rich fission fragments generated by the heavy fissionable isotopes  $^{235}\text{U}$ ,  $^{238}\text{U}$ ,  $^{239}\text{Pu}$ , and  $^{241}\text{Pu}$  [3, 4, 5]. In 2011 improved calculations by Mueller *et al.* [6] and Huber [7] (HM model) predicted reactor antineutrino fluxes which are about 5% larger than the fluxes measured in several short-baseline reactor neutrino experiments. This discrepancy is known as the “reactor antineutrino anomaly” (RAA) [8].

There are two basic methods to calculate the predicted reactor antineutrino fluxes: the summation method and the conversion method [4, 5]. The summation method is based on fission and decay information provided by the nuclear databases. The conversion method utilizes virtual branches to convert measured  $\beta$  spectra to corresponding antineutrino spectra. The converted  $^{235}\text{U}$ ,  $^{239}\text{Pu}$ , and  $^{241}\text{Pu}$  antineutrino spectra are based on the measurement at the Institut Laue-Langevin (ILL) in the 1980’s [9]. The converted  $^{238}\text{U}$  antineutrino spectrum can be obtained based on the measured  $\beta$  spectrum at FRM II in Garching [10] in 2013. In addition to the HM model, we consider other three conversion models: HKSS [11], KI [12] and HKSS-KI models, and one summation model: EF [13] model.

Our updated calculation of IBD yields in all models is presented in Section 2, and then the methods of analysis are introduced in Section 3. Our results of the fits of reactor rates and evolution data are also shown in Section 4 and Section 5, respectively. In Section 6, we discuss which the best-fit model is. At last, we will summarize our conclusions.

## 2 Model predictions

The event rates are usually expressed as a physical quantity called “cross section per fission”  $\sigma_{f,a}$  as known as “inverse beta decay (IBD) yield”:



Content from this work may be used under the terms of the [Creative Commons Attribution 3.0 licence](https://creativecommons.org/licenses/by/3.0/). Any further distribution of this work must maintain attribution to the author(s) and the title of the work, journal citation and DOI.

$$\sigma_{f,a} = \sum_i f_i^a \sigma_i, \quad \text{with} \quad \sigma_i = \int_{E_\nu^{\text{thr}}}^{E_\nu^{\text{max}}} dE_\nu \Phi_i(E_\nu) \sigma_{\text{IBD}}(E_\nu) \quad (1)$$

where  $a$  is the experiment label,  $\sigma_i$  is the IBD yield for the fissionable isotope  $i$ , and  $f_i^a$  is the effective fission fraction of the isotope  $i$ .  $\Phi_i(E_\nu)$  is the neutrino flux generated by the fissionable isotope  $i$ , and  $\sigma_{\text{IBD}}(E_\nu)$  is the IBD cross section considered as the Strumia and Vissani cross section [14] including the radiative corrections with PDG2020 [2] here. The neutrino energy is integrated from  $E_\nu^{\text{thr}} = 1.806 \text{ MeV}$  to  $E_\nu^{\text{max}} = 10 \text{ MeV}$  using the EF model high-energy spectra with conservative 100% uncertainties. The off-equilibrium corrections are also taken into account, which is based on Table VII of Ref. [6] assuming the 450 days approximation of the spectrum at equilibrium. Our updated results of IBD yields for these five models are shown in Table 1.

**Table 1.** Our estimations of the theoretical IBD yields of the four fissionable isotopes in units of  $10^{-43} \text{ cm}^2/\text{fission}$  predicted by different models.

Model	$\sigma_{235}$	$\sigma_{238}$	$\sigma_{239}$	$\sigma_{241}$
<b>HM</b>	$6.74 \pm 0.17$	$10.19 \pm 0.83$	$4.40 \pm 0.13$	$6.10 \pm 0.16$
<b>EF</b>	$6.29 \pm 0.31$	$10.16 \pm 1.02$	$4.42 \pm 0.22$	$6.23 \pm 0.31$
<b>HKSS</b>	$6.82 \pm 0.18$	$10.28 \pm 0.84$	$4.45 \pm 0.13$	$6.17 \pm 0.16$
<b>KI</b>	$6.41 \pm 0.14$	$9.53 \pm 0.48$	$4.40 \pm 0.13$	$6.10 \pm 0.16$
<b>HKSS-KI</b>	$6.48 \pm 0.14$	$10.28 \pm 0.84$	$4.45 \pm 0.13$	$6.17 \pm 0.16$

### 3 Method of analysis

A  $\chi^2$  function based on Wilks' theorem is usually applied to analyze the reactor antineutrino data. There are three main approaches when choosing different methods to deal with systematic theoretical uncertainties: **(A)** consider a covariance matrix with experimental and theoretical uncertainties added in quadrature [8]; **(B)** calculate the fit results considering only the experimental uncertainties and add by hand a global theoretical uncertainty [15]; **(C)** take into account the theoretical uncertainties with appropriate pull terms [16].

Method **(A)** suffers the “Peelle’s Pertinent Puzzle” (PPP) [17] due to discrepant and strongly correlated data. Method **(B)** avoids PPP, but it requires the estimation of a global theoretical uncertainty by hand, which seems impossible. Method **(C)** avoids PPP by decoupling the minimization of the  $\chi^2$  function with respect of the physical parameters from the pull coefficients:

$$\chi^2 = \sum_{a,b} \left( \sigma_{f,a}^{\text{exp}} - R_{\text{NP}}^a \sigma_{f,a}^{\text{th}} \right) (V^{\text{exp}})^{-1}_{ab} \left( \sigma_{f,b}^{\text{exp}} - R_{\text{NP}}^b \sigma_{f,b}^{\text{th}} \right) + \sum_{i,j} (r_i - 1) \left( \tilde{V}^{\text{mod}} \right)_{ij}^{-1} (r_j - 1), \quad (2)$$

$$\sigma_{f,a}^{\text{th}} = \sum_i r_i f_i^a \sigma_i^{\text{mod}}. \quad (3)$$

Here  $\sigma_i^{\text{mod}}$  denotes the IBD yield of the antineutrino flux generated by the fissionable isotope  $i$  and  $\tilde{V}_{ij}^{\text{mod}} = V_{ij}^{\text{mod}} / (\sigma_i^{\text{mod}} \sigma_j^{\text{mod}})$ , where  $V^{\text{mod}}$  is the covariance matrix. The coefficient  $R_{\text{NP}}^a$  is a possible suppression factor of the IBD yield in the experiment  $a$ .

**Table 2.** Average ratio  $\bar{R}_{\text{mod}}$  obtained from the least-squares analysis of the reactor rates in Table IV of Ref. [1] and of the Daya Bay [18] and RENO [19] evolution data.

Model	Rates		Evolution		Rates + Evolution	
	$\bar{R}_{\text{mod}}$	RAA	$\bar{R}_{\text{mod}}$	RAA	$\bar{R}_{\text{mod}}$	RAA
<b>HM</b>	$0.936^{+0.024}_{-0.023}$	$2.5\sigma$	$0.933^{+0.025}_{-0.024}$	$2.6\sigma$	$0.930^{+0.024}_{-0.023}$	$2.8\sigma$
<b>EF</b>	$0.960^{+0.033}_{-0.031}$	$1.2\sigma$	$0.975^{+0.032}_{-0.030}$	$0.8\sigma$	$0.975^{+0.032}_{-0.030}$	$0.8\sigma$
<b>HKSS</b>	$0.925^{+0.025}_{-0.023}$	$2.9\sigma$	$0.925^{+0.026}_{-0.024}$	$2.8\sigma$	$0.922^{+0.024}_{-0.023}$	$3.0\sigma$
<b>KI</b>	$0.975^{+0.022}_{-0.021}$	$1.1\sigma$	$0.973^{+0.023}_{-0.022}$	$1.2\sigma$	$0.970 \pm 0.021$	$1.4\sigma$
<b>HKSS-KI</b>	$0.964^{+0.023}_{-0.022}$	$1.5\sigma$	$0.955^{+0.024}_{-0.023}$	$1.9\sigma$	$0.960^{+0.022}_{-0.021}$	$1.8\sigma$

#### 4 Fit of reactor rates

In this section, we consider the data listed in Table IV of Ref. [1]. Figure 1 shows the ratios of measured and expected rates for the reactor experiments for HM model:  $\bar{R}_{\text{HM}} = 0.936^{+0.024}_{-0.023}$ , which indicates a RAA with  $2.5\sigma$ . HKSS model gives a reactor antineutrino anomaly  $2.9\sigma$ .

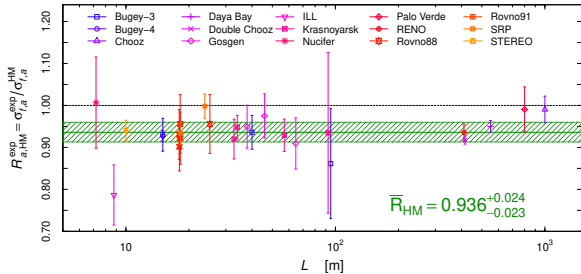


**Figure 1.** Ratio  $R_{a, \text{HM}}^{\text{exp}}$  of measured and expected IBD yields for the reactor experiments considered in our analysis as a function of the reactor-detector distance  $L$  for the HM model. The error bars show the experimental uncertainties. The horizontal green band shows the average ratio  $\bar{R}_{\text{HM}}$  and its uncertainty, that gives a  $2.5\sigma$  RAA.

There is practically no RAA for the EF model, since  $\bar{R}_{\text{EF}}$  differs from unity by only  $1.2\sigma$ . Also the KI corrections lead to the practical disappearance of RAA, especially without the HKSS corrections. However, as for the 5 MeV bump, it is not fitted well by any of the models. Since the HKSS corrections give only a partial explanation of the 5 MeV bump, the problem of the calculation of the reactor antineutrino spectra needs further studies.

#### 5 Fit of reactor fuel evolution data

The Daya Bay [18] and RENO [19] collaborations have published measurements of the IBD yield during the evolution of the reactor fuel. To compare these flux evolution data with the different model predictions, we first fit the evolution data with a linear function describing the IBD yield as a function of  $f_{239}$ , as done by the Daya Bay [18] and RENO [19] collaborations:

$$\sigma_{f,a}^{\text{lin}} = \bar{\sigma}_f + \frac{d\sigma_f}{df_{239}} (f_{239}^a - \bar{f}_{239}), \quad (4)$$

where  $\bar{\sigma}_f$  is the average IBD yield and  $d\sigma_f/df_{239}$  is the change in the IBD yield. The discrepancies of  $d\sigma_f/df_{239}$  shown in Figure 2(b) are  $3.5\sigma$  and  $3.6\sigma$  for the HM model and HKSS model, respectively. However, other models give consistent values of  $\bar{\sigma}_f$  and  $d\sigma_f/df_{239}$ .

Then, we also fit the evolution data and the combined data using Eq. 2 as done in Section 4. In Table 2, the inclusion of the evolution data confirms the existence of a reactor antineutrino anomaly for the HM ( $2.8\sigma$ ) and HKSS ( $3.0\sigma$ ) models and the absence of the anomaly for the EF model (only  $0.8\sigma$ ). For KI and HKSS-KI models, the resulting  $1.4\sigma$  (KI) and  $1.8\sigma$  (HKSS-KI) are still too small to claim an anomaly.

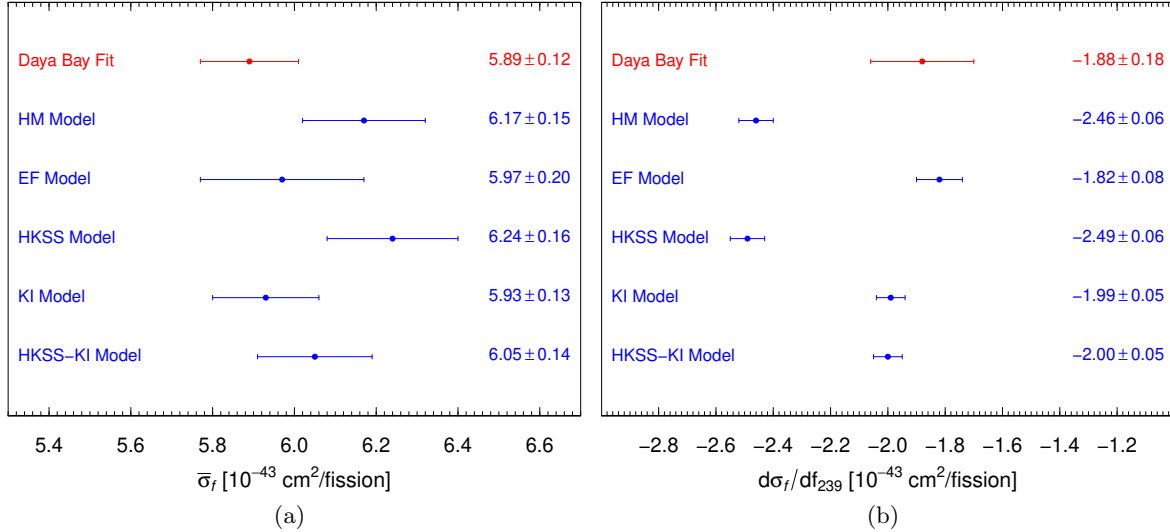


**Figure 2.** Results of the linear fits of the Daya Bay [18] evolution data.

## 6 Best-fit reactor flux model

In this section we apply goodness of fit tests to the reactor rates to select which the best-fit model is. If the fluctuations of the data with respect to the model prediction are Gaussian, the probability distribution function is given by

$$p(\sigma_{f,1}^{\text{exp}}, \dots, \sigma_{f,N}^{\text{exp}}) = \frac{e^{-\chi_{\text{tot}}^2/2}}{\sqrt{(2\pi)^N |V^{\text{tot}}|}}, \quad (5)$$

$$\chi_{\text{tot}}^2 = \sum_{a,b} \left( \sigma_{f,a}^{\text{exp}} - \sigma_{f,a}^{\text{mod}} \right) (V^{\text{tot}})^{-1}_{ab} \left( \sigma_{f,b}^{\text{exp}} - \sigma_{f,b}^{\text{mod}} \right), \quad (6)$$

where  $N$  is the number of data points and  $V^{\text{tot}}$  is the total covariance matrix.

Table 3 shows that the standard  $\chi^2$  goodness of fit test rejects none of the five models if we consider the usual minimum  $p$ -value of 5% corresponding to a confidence level of 95%. However, the  $\chi^2$  test is only sensitive to the sizes not the signs of the deviations. In order to perform statistical tests that probe the Gaussian distribution of the data taking into account the signs of the deviations from the model predictions, we should consider the transformed data  $x_a^{\text{mod}}$

$$x_a^{\text{mod}} = \sum_b (V^{\text{tot}})^{-1/2}_{ab} \left( \sigma_{f,b}^{\text{exp}} - \sigma_{f,b}^{\text{mod}} \right), \quad (7)$$

that should have a Gaussian distribution with zero mean and unit standard deviation. We first checked with the Shapiro-Wilk test (SW) that  $x_a^{\text{mod}}$  have an empirical Gaussian distribution. Then, we applied the following tests: sign, Kolmogorov-Smirnov (KS), Cramer-von Mises (CVM), Anderson-Darling (AD),  $Z_K$ ,  $Z_C$ , and  $Z_A$  tests, which are sensitive to the sign and size of the deviations of the transformed data with respect to the standard Gaussian distribution.

Since the EF and KI models are preferred by different tests and sets of data, it is fair to consider both as favorite. Therefore, we conclude that the KI model is the best among the conversion models and the only summation model that we considered, the EF model, is practically equally good.

**Table 3.** *p*-values of goodness of the fit tests of the combined data for the five models.

Test	HM	EF	HKSS	KI	HKSS-KI
<b>Rates + Evolution</b>					
<b><math>\chi^2</math></b>	0.13	0.22	0.08	0.68	0.44
<b>SW</b>	0.32	0.13	0.35	0.59	0.41
<b>sign</b>	0.03	0.38	0.006	0.38	0.11
<b>KS</b>	0.04	0.84	0.02	0.39	0.20
<b>CVM</b>	0.02	0.67	0.006	0.38	0.14
<b>AD</b>	0.02	0.57	0.006	0.40	0.13
<b><math>Z_K</math></b>	$< 10^{-3}$	0.05	$< 10^{-3}$	0.05	0.008
<b><math>Z_C</math></b>	0.02	0.11	0.005	0.55	0.15
<b><math>Z_A</math></b>	0.03	0.20	0.01	0.41	0.12
<b>weighted average</b>	0.05	0.35	0.03	0.42	0.16

## 7 Summary and conclusions

In Ref. [1] we revisited the reactor antineutrino anomaly based on the recent reactor antineutrino flux calculations. We first performed an improved calculation of the IBD yields of five reactor antineutrino flux models in Section 2. Then, based on the proper statistical method for the analysis discussed in Section 3, we calculated the suppression of the reactor antineutrino flux predicted by the 5 models by fitting the measured rates listed in Table IV of Ref. [1]. We found there is practically no anomaly for the EF, KI, and HKSS-KI models. In Section 5, the addition of the Daya Bay [18] and RENO [19] evolution data confirms these conclusions. In Section 6, we further explored the question of which is the best-fit model by applying several goodness of fit tests. We can consider EF as the best summation model and KI as the best conversion model, leaving the decision of a clear preference between the two models to future studies with more data.

## References

- [1] Giunti C, Li Y F, Ternes C A and Xin Z 2021 (*Preprint* 2110.06820)
- [2] Zyla P *et al.* (Particle Data Group) 2020 *PTEP* **2020** 083C01
- [3] Bemporad C, Gratta G and Vogel P 2002 *Rev. Mod. Phys.* **74** 297 (*Preprint* hep-ph/0107277)
- [4] Huber P 2016 *Nucl. Phys.* **B908** 268–278 (*Preprint* arXiv:1602.01499)
- [5] Hayes A C and Vogel P 2016 *Ann. Rev. Nucl. Part. Sci.* **66** 219–244 (*Preprint* arXiv:1605.02047)
- [6] Mueller T A *et al.* 2011 *Phys. Rev.* **C83** 054615 (*Preprint* arXiv:1101.2663)
- [7] Huber P 2011 *Phys. Rev.* **C84** 024617 (*Preprint* arXiv:1106.0687)
- [8] Mention G *et al.* 2011 *Phys. Rev.* **D83** 073006 (*Preprint* arXiv:1101.2755)
- [9] Von Feilitzsch F, Hahn A A and Schreckenbach K 1982 *Phys. Lett.* **B118** 162–166
- [10] Haag N, Gutlein A *et al.* 2014 *Phys. Rev. Lett.* **112** 122501 (*Preprint* arXiv:1312.5601)
- [11] Hayen L *et al.* 2019 *Phys. Rev.* **C100** 054323 (*Preprint* arXiv:1908.08302)
- [12] Kopeikin V, Skorokhvatov M and Titov O (*Preprint* arXiv:2103.01684)
- [13] Estienne M, Fallot M *et al.* 2019 *Phys. Rev. Lett.* **123** 022502 (*Preprint* arXiv:1904.09358)
- [14] Strumia A and Vissani F 2003 *Phys. Lett.* **B564** 42 (*Preprint* astro-ph/0302055)
- [15] An F *et al.* (Daya Bay) 2017 *Chin. Phys.* **C41** 013002 (*Preprint* arXiv:1607.05378)
- [16] Giunti C, Ji X P, Laveder M, Li Y F and Littlejohn B R 2017 *JHEP* **1710** 143 (*Preprint* arXiv:1708.01133)
- [17] 1987 R.W. Peelle, Oak Ridge National Laboratory Informal Memorandum, 1987
- [18] An F P *et al.* (Daya Bay) 2017 *Phys. Rev. Lett.* **118** 251801 (*Preprint* arXiv:1704.01082)
- [19] Bak G *et al.* (RENO) 2019 *Phys. Rev. Lett.* **122** 232501 (*Preprint* arXiv:1806.00574)